24th INTERNATIONAL CONGRESS ON SOUND AND VIBRATION
23–27 July 2017, London

ROBUST FEEDBACK CONTROL OF THERMOACOUSTIC OSCILLATIONS

Alessandro Orchini
University of Cambridge, Engineering Department, Trumpington Street, Cambridge, UK
email: aorchini@ic.ac.uk
Simon J. Illingworth
University of Melbourne, Mechanical Engineering Department, VIC 3010, Melbourbe, Australia

This study investigates the feedback control of nonlinear thermoacoustic oscillations. A particular aim is to investigate the efficacy of feedback control when the system's nonlinear dynamics are rich. The flame is modelled by the kinematic G-equation. The acoustic model is based on the experimental geometry of R. Balachandran [1], accounting for a spatially non-uniform unsteady flow field and curvature corrections on the flame speed. Crucially, we see that both the gain and the phase vary with the forcing amplitude. This means that, when the flame dynamics is coupled with the acoustic response of the combustor, bifurcations of both the supercritical and subcritical type are possible. This coupled system is in turn coupled to a feedback controller, whose objective is to completely eliminate oscillations. Robust control techniques are used to design the controller, which is then applied to both the linear and fully nonlinear system. Our analysis highlights how controllers designed on the linear flame response (FTF) fail in stabilising thermoacoustic oscillations due to subcritical phenomena. On the other hand, controllers designed on the nonlinar flame response (FDF) are more robust in that they can control oscillations arising because of both super- and subcritical bifurcations.
Keywords: thermoacoustics, control, nonlinear, Describing Function

Introduction

Thermoacoustic oscillations can occur whenever combustion takes place inside an acoustic resonator. Unsteady combustion is an efficient acoustic source, and combustors tend to be highly resonant systems. Therefore, for suitable phase between unsteady combustion and acoustic perturbations, large-amplitude self-excited oscillations can occur. Most recent studies of combustion oscillations have focused on low NO_x premixed gas turbine combustors, which are particularly susceptible to thermoacoustic instability [2]. These studies typically assume linear acoustics: the low Mach number means that the acoustic pressure fluctuations are small even when the acoustic velocity fluctuations are large [3]. The heat release is therefore treated as the only nonlinear element in the coupled system.

When a thermoacoustic system is unstable, oscillations grow in amplitude, and typically saturate to a periodic motion known as a limit cycle. Fig. 1 shows the steady state amplitude, a, for two types of nonlinear behaviour that can be observed in linearly unstable thermoacoustic systems. The first is a supercritical Hopf bifurcation, in which the limit cycle amplitude grows gradually as the control parameter, P, increases past P_c which is the critical point through which the linear stability of the system changes. The second is a subcritical bifurcation, in which the limit cycle amplitude grows suddenly as P increases past P_c, and for which there are two stable solutions in the region between P_f (the fold point) and P_c. This is known as the bistable region: even if the system is linearly stable, a strong enough perturbation can trigger large amplitude oscillations.

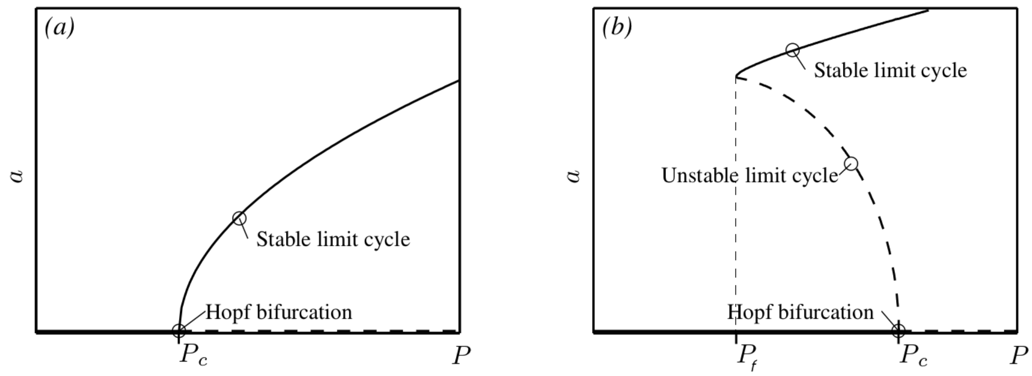

Figure 1: The limit cycle amplitude, a, as a function of a control parameter, P, for (a) a supercritical bifurcation and (b) a subcritical bifurcation. At the critical value P_c a Hopf bifurcation occurs, and the system becomes linearly unstable. P_f is the fold point in a subcritical bifurcation, below which no oscillations can be sustained. The parameter region enclosed between P_f and P_c is bistable.

The frequency and amplitude of limit cycles arising from both super- and subcritical Hopf bifurcations can be found in the frequency domain using a Flame Describing Function (FDF) and the harmonic balance method [4, 5]. This involves measuring the flame's response to harmonic forcing for different forcing frequencies and forcing amplitudes. By assuming that the flame's response to a given forcing frequency is predominately at that frequency (*i.e.*, by discarding higher harmonics using the so-called filtering hypothesis [6]), the FDF provides the flame's gain and phase as a function of forcing frequency and forcing amplitude. Dowling [7] calculated the FDF for a kinematic model of a premixed ducted flame and found that the limit cycle amplitude of the coupled system was determined by the amplitude-dependence of the gain. Noiray *et al.* [4] measured the FDF of a premixed flame experimentally and found that the limit cycle amplitude of the coupled system was determined by the amplitude-dependence of both the gain and the phase of the flame's response.

As well as looking at the effect of a simple saturation nonlinearity on the dynamics of thermoacoustic oscillations, Dowling [3] also looked at implications for feedback control. It was found that a feedback controller designed on the linear response (FTF), as well as stabilising the linear system, was also stabilising when applied from an already-established limit cycle. A Describing Function analysis was used to explain why the controller was still successful when applied to the limit-cycling system. It is important to remember here that, due to the relatively simple nature of the flame's nonlinearity, there was no amplitude dependence of the flame's phase response, and therefore the subcritical bifurcations shown in Fig. 1 (b) could not occur. In more recent work, the amplitude dependence of the flame's phase response has been shown to play an important role for the dynamics of the coupled system. In particular, the subcritical bifurcations depicted in Fig. 1 (b) can occur. A recent study showed that, using $\mathcal{H}_\infty$ loop-shaping techniques, one can guarantee that a controller designed on a certain amplitude level will be able to stabilise the system at other amplitudes, too [8]. Our aim here is to investigate the efficacy of feedback control when the system's nonlinear dynamics are rich. We find that controllers designed using the FTF only, although able to stabilise oscillations arising from supercritical bifurcations, will fail in stabilising limit cycle oscillations arising from subcritical bifurcations. On the other hand, controllers designed using the FDF are more robust and can stabilise oscillations arising from both types of bifurcations.

Thermoacoustic modelling

Acoustics

The acoustic configuration examined in this study is based on the experimental geometry of Balachandran *et al.* [1], and is shown in Fig. 2. We account for mean flow effects, area/temperature

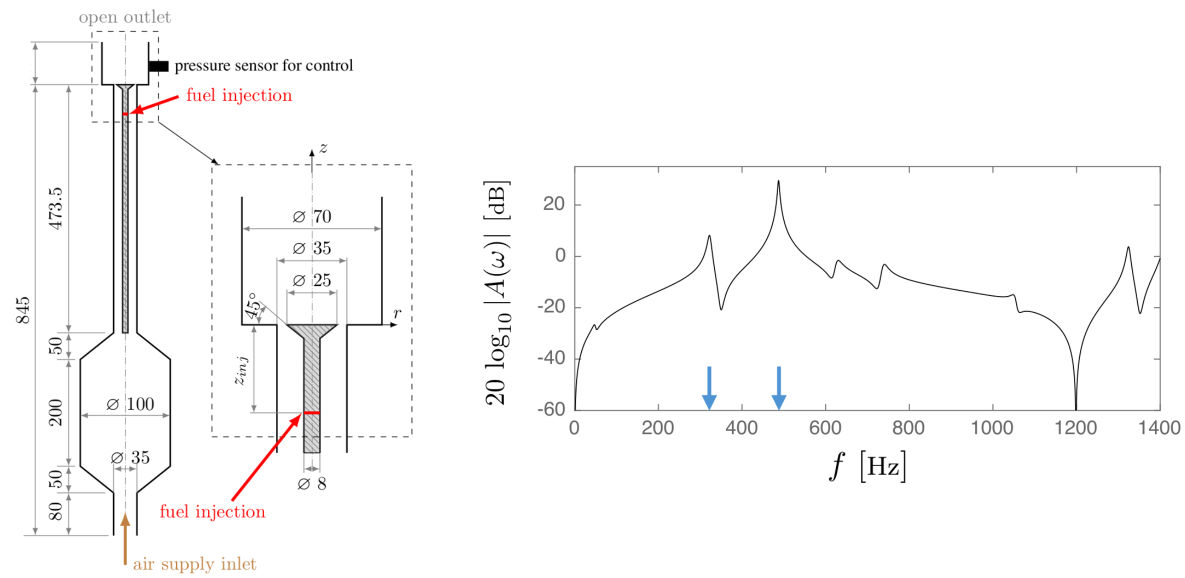

Figure 2: Left: schematic of the acoustic network modelled using LOTAN. Right: acoustic velocity response at the flame location to heat release perturbations. The frequencies of two acoustic modes are highlighted.

changes across the combustor, and we use simple models for the acoustic reflection coefficients at the inlet (closed) and outlet (open, with corrections). The geometry is implemented using LOTAN [9]. The acoustic response of the geometry to heat release perturbations is extracted and fit onto a state-space model, using the procedure described in [5]. This is shown in Fig 2, where the frequencies of the first two acoustic modes are highlighted. When coupling the acoustics with the flame (see next sections), we find that thermoacoustic oscillations always occur at frequencies close to those of these acoustic modes.

Flame

The flame dynamics chosen to close the thermoacoustic feedback loop in our system is that of a laminar, conical flame. This is because low-order models for the turbulent flame that stabilise in the combustor shown in Fig. 2 are still being developed. The G-equation model for a laminar conical flame, instead, is well established in the literature [10], and contains all the features we are looking for here, *i.e.*, a variation of both the gain and phase flame responses with respect to the forcing amplitude $a \equiv A/\overline{u}$, where A and $\overline{u}$ are the dimensional values of the perturbation and mean flow velocities, respectively. The numerical method used to simulate the flame dynamics is the same of that described in [5]. The Flame Describing Function for this model (gain and phase) is obtained by forcing the flame base with a sinusoidal input $u'/\overline{u} = a\sin(\omega t)$, and varying the values of both the amplitude a and frequency $f = \omega/(2\pi)$ over wide ranges.

The resulting Flame Describing Function, defined as

$$\mathcal{F}(\omega, a) \equiv \frac{\hat{q}_1(\omega, A)}{\overline{Q}}\frac{\overline{u}}{A} \tag{1}$$

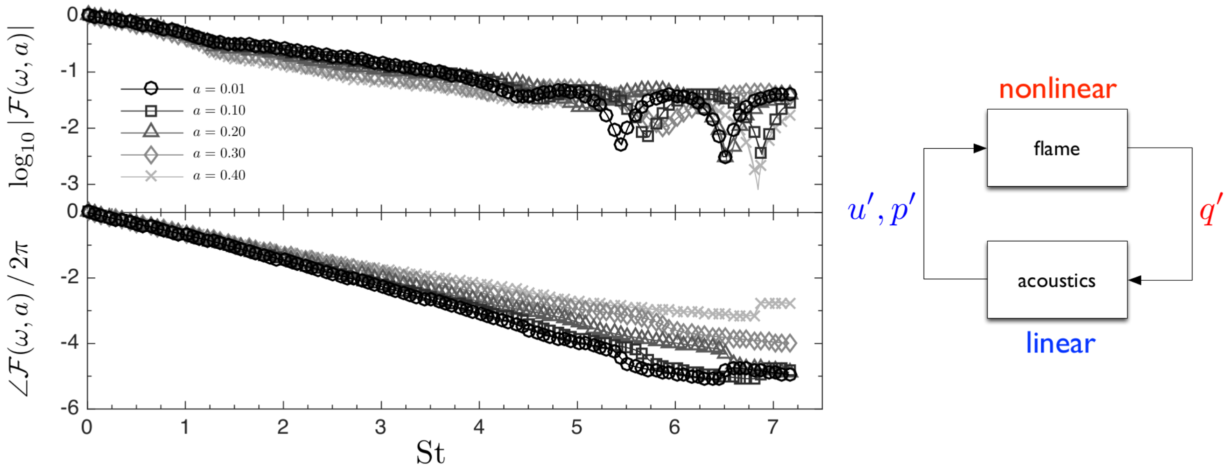

Figure 3: Left: the Flame Describing Function, $\mathcal{F}(s, a)$, for five forcing amplitudes: gain (top) and phase (bottom). Right: closed loop thermoacoustic feedback loop. In our model, only u' affects the flame dynamics. We will however use p' to actuate the controller.

is plotted in Fig. 3. Because both the gain and the phase vary with forcing amplitude, bifurcations of both the supercritical and subcritical type are possible (see Fig. 1).

Stability map

By coupling the acoustic velocity response to the FDF as shown in Fig. 3 (b), we can generate a stability map as the one shown in Fig. 4 We find that only two modes can have a positive growth

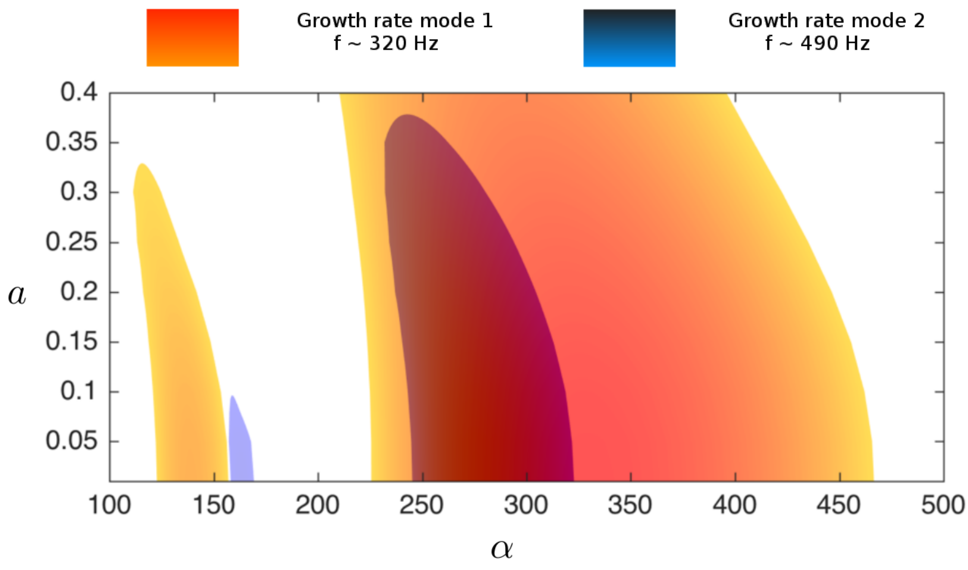

Figure 4: Stability maps of the closed-loop thermoacoustic systems. The bifurcation parameters α varies the size of the flame of the acoustics with respect to the flame. Colours highlight the regions in which (at least) a thermoacoustic mode has a positive growth rate. Both super- and subcritical phenomena can be observed.

rate; they have frequencies close to those of the first two acoustic modes of the combustor. We have highlighted with colours the regions in which these thermoacoustic modes have positive growth rates. The bifurcation parameter used, $\alpha \equiv \tau_{fl}/\tau_{ac}$, is the ratio between the flame time scale $\tau_{fl} \equiv L_f/\overline{u}$ and the acoustic time scale $\tau_{ac} \equiv L/c$, where L_f is the flame length, L the combustor length, and c

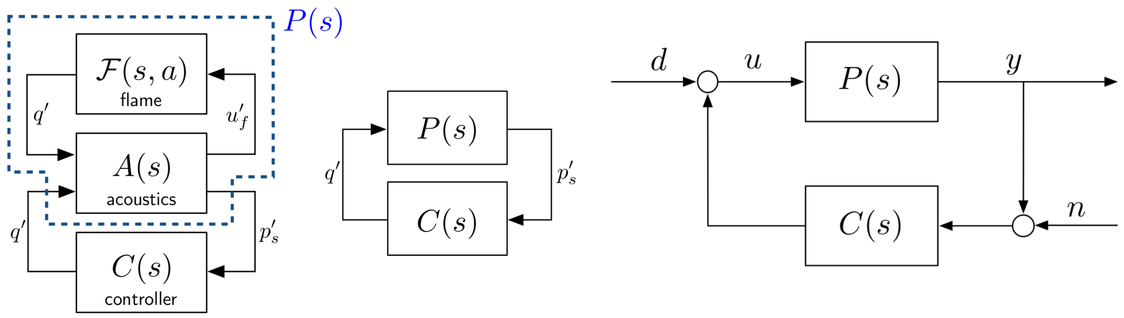

Figure 5: Sketch of the feedback control system. The thermo-acoustic response is combined in a single plant, P, to simplify the robust control analysis. On the right, arbitrary variable names are used for the input/outputs of the controlled system, and external disturbances (see eq. (6)).

the speed of sound. This was shown to be a key parameter in the stability of thermoacoustic systems in [11].

Let us now relate the Describing Function analysis (in particular, its description of the variations in the flame's gain and phase with forcing amplitude) to the supercritical and subcritical bifurcations seen in Fig. 1. If the flame's phase does not change with forcing amplitude, then one would expect to find only supercritical bifurcations (provided that the flame's gain decreases with increasing forcing amplitude, which is a sensible assumption). This is because as the forcing amplitude increases, the positive feedback between unsteady heat release and acoustics can only weaken, since the flame's gain is decreasing, while the phase between them remains fixed. If both the gain and the phase vary, however, then both supercritical and subcritical bifurcations are possible. In this case, even if we assume that the flame's gain decreases with increasing forcing amplitude as before, variations in phase can actually lead to stronger positive feedback between unsteady heat release and acoustics.

This is indeed what we observe from Fig. 4: for example, at $\alpha = 140$ the system is linearly unstable, and oscillations with a frequency of about 320 Hz will grow and saturate at an amplitude $a \approx 0.2$. On the other hand, at $\alpha = 120$, the system is linearly stable; however, perturbing the system with a signal having $a \gtrsim 0.15$, triggers subcritical phenomena and an instability arises which saturates at an amplitude $a \approx 0.3$. This is consistent with experimental observations in which the experimentally-determined FDF exhibits significant changes in both gain and phase, as the one discussed in [4].

Controller design

Our task, therefore, is to design a controller that is sufficiently robust to provide closed-loop stability even in the presence of the flame's changes in gain and phase, and predict the changes in the dynamics of the coupled system that this will cause. This is shown in Fig. 5 (a): the coupled thermoacoustic system is represented by the two lower blocks. Notice that the flame dynamics, $\mathcal{F}(s, a)$, is a function of both the Laplace variable, s, and the forcing amplitude, a. The feedback controller (top block in Fig. 5 (a)) is denoted by $C(s)$ and is designed using robust control techniques [12] to stabilise both the linear and fully nonlinear system.

To do so we will employ model-based linear control. There exist many methods for designing linear controllers based on linear models. These include classical loop-shaping; pole placement methods; Linear Quadratic and Linear Quadratic Gaussian control; and $\mathcal{H}_2$- and $\mathcal{H}_\infty$-based methods. The method chosen here is $\mathcal{H}_\infty$ loop-shaping [13, 8], a modern synthesis method which is well-favoured in the control community. A particular strength is the way in which it consolidates classical control with modern control in a powerful and pleasing way [12].

In order to introduce the method, we must first do three things: (i) define a state-space model; (ii) move into the frequency domain; (iii) introduce the $\mathcal{H}_\infty$-norm. Consider a linear, time-invariant dynamical system given in state-space form as

$$\begin{aligned}\dot{\boldsymbol{x}}(t) &= A\boldsymbol{x}(t) + B\boldsymbol{u}(t)\\ \boldsymbol{y}(t) &= C\boldsymbol{x}(t) + D\boldsymbol{u}(t),\end{aligned} \tag{2}$$

where $\boldsymbol{u} \in \mathbb{R}^p$ is a vector of inputs, $\boldsymbol{y} \in \mathbb{R}^q$ is a vector of outputs, $\boldsymbol{x} \in \mathbb{R}^n$ is the system state of dimension n, and A, B, C and D are suitably-dimensioned matrices.

Taking Laplace transforms of (2) and rearranging, we arrive at the transfer function, $P(s)$, defined by $\boldsymbol{y}(s) = P(s)\boldsymbol{u}(s)$, with

$$P(s) \equiv C(sI - A)^{-1}B + D. \tag{3}$$

For p inputs and q outputs, $P(s)$ is a matrix of dimension $q \times p$. We can now introduce the $\mathcal{H}_\infty$ norm of a transfer function, which is defined for stable systems as

$$\|P\|_\infty \equiv \max_\omega \bar{\sigma}(P(j\omega)). \tag{4}$$

That is, an input that comes arbitrarily close to attaining the $\mathcal{H}_\infty$ norm concentrates its energy at the frequency where the gain of the system—as measured by the maximum singular value of its frequency response matrix—is largest. In the time domain this means that

$$\|P\|_\infty = \sup_{u \neq 0} \frac{\|P\boldsymbol{u}\|_2}{\|\boldsymbol{u}\|_2}. \tag{5}$$

$\mathcal{H}_\infty$ loop shaping

Having moved into the frequency domain and defined the $\mathcal{H}_\infty$ norm, we now define the standard feedback arrangement considered in the $\mathcal{H}_\infty$ loop-shaping method, together with the quantity $b_{P,C}$ used to characterize it:

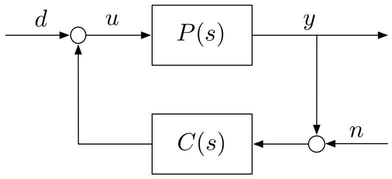

$$b_{P,C} \equiv \left\| \begin{bmatrix} P \\ I \end{bmatrix} (I - CP)^{-1} \begin{bmatrix} -C & I \end{bmatrix} \right\|_\infty^{-1}. \tag{6}$$

Here d represents disturbances at the input and n represents sensor noise at the output. Note that the expression given for $b_{P,C}$ is valid only if the feedback interconnection of P and C is stable, otherwise, $b_{P,C} = 0$.

$b_{P,C}$ is therefore the inverse of the $\mathcal{H}_\infty$ norm from disturbances d and noise n to $\boldsymbol{u}$ and $\boldsymbol{y}$ in the standard feedback configuration shown above. The norm cannot be made smaller than 1, which means that, for any P and C, $b_{P,C}$ lies in the range $[0, 1]$. A simple interpretation of $b_{P,C}$ is as follows: a large value of $b_{P,C}$ implies that the $\mathcal{H}_\infty$ norm of the transfer function matrix in (6) remains small over all frequencies and all directions. The use of $b_{P,C}$ as a performance measure is therefore motivated by the fact that it bounds the gain of all four closed-loop transfer functions at any point in the loop. Furthermore, for single-input-single-output systems, the classical gain and phase margins of the closed-loop can be related to $b_{P,C}$, providing an important and pleasing link to classical control. Glover & McFarlane [14] show that $b_{P,C}$ can be maximized over all stabilising C to give

$$b_{\text{opt}}(P) = \sup_C b_{P,C}, \tag{7}$$

and this is the optimization that the $\mathcal{H}_\infty$ loop-shaping procedure achieves.

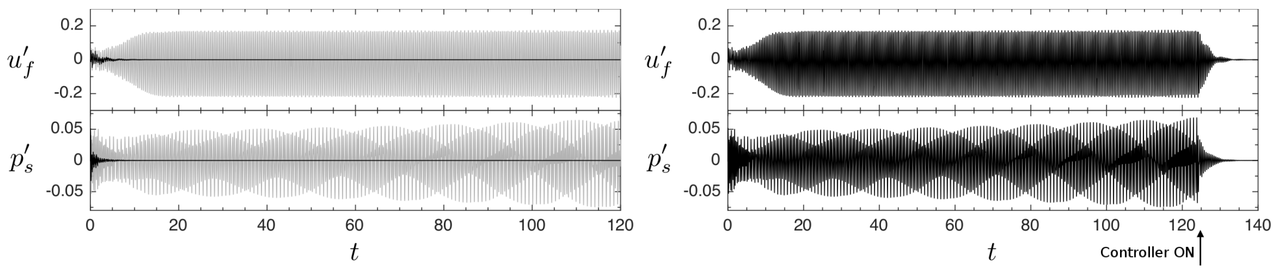

Figure 6: Supercritical results ($\alpha = 140$): a controller designed on the FTF is able to stabilise either starting from fixed point (left) or limit cycle (right) conditions. In grey, the time evolution of velocity/pressure when the controller is absent. In black, the behaviour of the system when the controller is on (or switched on after a time interval).

Results

Supercritical case

We start choosing $\alpha = 140$. Performing time domain simulations, with the same procedure as that described in [5], we find that, consistently with the frequency domain analysis shown in Fig. 4, the uncontrolled system is unstable, and the amplitude of the acoustic velocity fluctuations saturates at an amplitude $a \approx 0.2$, as shown in Fig. 6. Also the frequency of the steady state oscillations accurately matches the one predicted with the harmonic balance method. For this case, we find that designing the controller using the FTF only is good enough to stabilise the thermoacoustic system from both the fixed point (infinitesimally small amplitude) and from the limit cycle (finite amplitude). This is because the closed-loop growth rate predicted by the harmonic balance method monotonically decreases with the amplitude at this value of α (as was for [3]). Therefore the linear limit is the most unstable situation: designing a controller on the linear response is sufficient to guarantee stabilisation also from limit cycle conditions.

Subcritical case

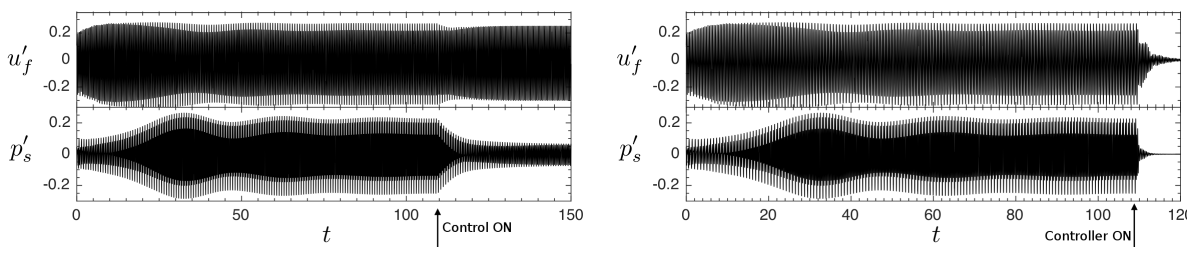

Figure 7: Subcritical results ($\alpha = 120$): a controller designed on the FTF is unaware of possible triggering phenomena, and cannot stabilise the oscillations (left). On the other hand, a controller which is guaranteed to be robust across the entire FDF achieves much better performance (right).

When α is chosen to be 120, instead, the system is bistable. It is linearly stable, but a large enough perturbation triggers finite amplitude oscillations. Designing the controller from the FTF is not good enough to stabilise the oscillation from limit cycle, as shown in Fig. 7, left. This is because the (linear) closed-loop system is not "aware" that the pole with frequency 320 Hz is potentially dangerous. However, by designing the controller so that it is robust across the entire FDF (see previous section and [8]), the controller becomes "aware" of subcritical pheonomea and is able to stabilise also oscillations arising from triggering effects, as shown in Fig. 7, right.

Conclusions

In this study, robust feedback control of thermoacoustic oscillations has been considered. A procedure similar to that outline in [8] has been followed to design controllers which are guaranteed to perform across the entire FDF amplitude range (evaluated numerically using a G-equation model). However, in contrast to [8], here emphasis is put on when such an analysis is necessary. Using a dynamical system perspective, we differentiate between two scenarios. The first is the supercritical case, in which the system is linearly unstable and the harmonic balance procedure predicts the growth rate to monotonically decrease with the oscillation amplitude level. This case was already considered by [3], and we verify that no robust control techniques are required, as the controller designed on the FTF is able to stabilise also large amplitude oscillations. The second possibility is the subcritical case, in which the system is bistable. Here the FTF information only is insufficient to design effective controllers. This is because the FTF predicts the system to be linearly stable, but ignores that finite amplitude perturbations may still trigger self-sustained oscillations. We find that, in this scenario, a controller designed on the FTF is unable to stabilise these triggered oscillations. On the other hand, a controller designed on the entire FDF using $\mathcal{H}_\infty$ techniques, is able to control also oscillations arising from subcritical phenomena.

References

1. Balachandran, R., Ayoola, B. O., Kaminski, C. F., Dowling, A. P. and Mastorakos, E. Experimental investigation of the nonlinear response of turbulent premixed flames to imposed inlet velocity oscillations, *Combust. Flame*, **143**, 37–55, (2005).
2. Richards, G. and Janus, M. Characterization of oscillations during premix gas turbine combustion, *J. Eng. Gas Turbines Power*, **120**, 294–302, (1998).
3. Dowling, A. P. Nonlinear self-excited oscillations of a ducted flame, *J. Fluid Mech.*, **346**, 271–290, (1997).
4. Noiray, N., Durox, D., Schuller, T. and Candel, S. A unified framework for nonlinear combustion instability analysis based on the Flame Describing Function, *J. Fluid Mech.*, **615**, 139–167, (2008).
5. Orchini, A., Illingworth, S. J. and Juniper, M. P. Frequency domain and time domain analysis of thermoacoustic oscillations with wave-based acoustics, *J. Fluid Mech.*, **775**, 387–414, (2015).
6. Gelb, A. and Velde, W. E. C., *Multiple-input describing functions and nonlinear system design* (1968).
7. Dowling, A. P. A kinematic model of a ducted flame, *J. Fluid Mech.*, **394**, 51–72, (1999).
8. Li, J. and Morgans, A. S. Feedback control of combustion instabilities from within limit cycle oscillations using $\mathcal{H}_\infty$ loop-shaping and the ν-gap metric, *Proc. of the Roy. Soc. A*, **472**, 20150821, (2016).
9. Stow, S. R. and Dowling, A. P. A time-domain network model for nonlinear thermoacoustic oscillations, *J. Eng. Gas Turbines Power*, **131**, 031502, (2009).
10. Preetham, Hemchandra, S. and Lieuwen, T. Dynamics of Laminar Premixed Flames Forced by Harmonic Velocity Disturbances, *J. Propul. Power*, **24**, 1390–1402, (2008).
11. Kashinath, K., Waugh, I. C. and Juniper, M. P. Nonlinear self-excited thermoacoustic oscillations of a ducted premixed flame: bifurcations and routes to chaos, *J. Fluid Mech.*, **761**, 1–26, (2014).
12. Vinnicombe, G., *Uncertainty and feedback: $\mathcal{H}_\infty$ loop-shaping and the ν-gap metric*, Imperial College Press (2000).
13. McFarlane, D. C. and Glover, K., *Robust controller design using normalized coprime factor plant descriptions*, Springer-Verlag (1990).
14. Glover, K. and McFarlane, D. Robust stabilization of normalized coprime factor plant descriptions with $\mathcal{H}_\infty$-bounded uncertainty, *IEEE Trans. Automat. Contr.*, **34** (8), 821–830, (1989).